

The Coronavirus Nucleocapsid Protein Is Dynamically Associated with the Replication-Transcription Complexes^{∇†}

Monique H. Verheije,^{1‡#} Marne C. Hagemeyer,^{1‡} Mustafa Ulasli,² Fulvio Reggiori,²
Peter J. M. Rottier,¹ Paul S. Masters,³ and Cornelis A. M. de Haan^{1*}

Virology Division, Department of Infectious Diseases and Immunology, Faculty of Veterinary Medicine, Utrecht University, Utrecht, Netherlands¹; Department of Cell Biology and Institute of Biomembranes, University Medical Centre Utrecht, Utrecht, Netherlands²; and David Axelrod Institute, Wadsworth Center, New York State Department of Health, Albany, New York³

Received 16 March 2010/Accepted 17 August 2010

The coronavirus nucleocapsid (N) protein is a virion structural protein. It also functions, however, in an unknown way in viral replication and localizes to the viral replication-transcription complexes (RTCs). Here we investigated, using recombinant murine coronaviruses expressing green fluorescent protein (GFP)-tagged versions of the N protein, the dynamics of its interactions with the RTCs and the domain(s) involved. Using fluorescent recovery after photobleaching, we showed that the N protein, unlike the nonstructural protein 2, is dynamically associated with the RTCs. Recruitment of the N protein to the RTCs requires the C-terminal N2b domain, which interacts with other N proteins in an RNA-independent manner.

All positive-strand RNA viruses assemble their replication complexes in association with intracellular membranes. Coronaviruses, enveloped plus-strand RNA viruses, induce in infected cells the formation of double-membrane vesicles (DMVs) and convoluted membranes (CMs). These structures harbor the nonstructural proteins (nsp's) (9, 14, 25, 26, 28) and are associated with viral RNA synthesis (1, 9, 20, 22). The nsp's, which jointly form the replication-transcription complexes (RTCs), presumably mediate the formation of these membranous structures by modifying endoplasmic reticulum-derived membranes and by recruiting cellular components to their need.

In addition to the nsp's, coronaviruses express several structural proteins, including at least the spike (S), envelope (E), membrane (M), and nucleocapsid (N) proteins (6). The N protein packages the viral genomic RNA to form the helical nucleocapsid that is incorporated into the budding particle but also fulfills additional roles during the viral infection. It has been shown to function as an RNA chaperone (33) and to facilitate viral RNA synthesis (2, 5, 16). Not surprisingly, the N protein localizes to DMVs and CMs, the sites where the RTCs are concentrated, in addition to the virion assembly sites (3, 7, 23, 28, 29). Furthermore, the nucleocapsid protein contributes to the perturbation of several host cellular processes (reviewed in reference 27).

Recently, we demonstrated that nsp2, once recruited to the RTCs, is not exchanged for nsp2 molecules present in the

cytoplasm and in other DMVs/CMs. That is, no recovery of fluorescence was observed when (part of) the nsp2-positive foci were photobleached (10). Whether the other nsp's or the N protein pool associated with the RTCs also lacks mobility at these sites remains unknown. Of particular interest are the dynamics of the N protein, as it is involved in different, spatially and temporally separated steps of the viral life cycle. We hypothesized that the N protein is not permanently bound to the RTCs but rather possesses a manifest intracellular mobility, as it is probably not involved only in viral RNA synthesis but also in its transport from the site of synthesis to the virion assembly sites, where it participates in virion assembly.

To test our hypothesis, we studied the dynamics of the N protein localized at the RTCs by live-cell imaging. To this end, we generated a recombinant mouse hepatitis coronavirus (MHV) expressing an additional copy of the N protein C-terminally fused to green fluorescent protein (N-GFP). The coding sequence for N-GFP was introduced into the viral genome as an additional expression cassette between genes 2a and S by targeted RNA recombination as previously described (18), thereby replacing the nonfunctional hemagglutinin-esterase gene (Fig. 1A). The resulting recombinant virus, MHV-N-GFP, was viable; however, it was rapidly outcompeted by viruses that had lost expression of the N fusion protein. As we were unable to demonstrate incorporation of N-GFP into progeny virions, we speculated that the fusion protein acts as a dominant negative during virion assembly. Of passage 2, approximately 10 to 20% of the virus population expressed detectable levels of N-GFP (data not shown), which was sufficient for our experimental goal.

To determine whether the N-GFP fusion protein, when expressed from the viral genome, was recruited to the RTCs, LR7 cells were inoculated with MHV-N-GFP, fixed at 6 h postinfection (p.i.), and subsequently processed for immunofluorescence analysis. The results show that the N-GFP was present throughout the cytoplasm at a low level and was concentrated in cytoplasmic foci that were colocalizing with the RTC protein markers nsp2/3 (antibody D4) and nsp8 (anti-p22

* Corresponding author. Mailing address: Virology Division, Department of Infectious Diseases & Immunology, Utrecht University, Yalelaan 1, 3584 CL Utrecht, Netherlands. Phone: 31 30 253 4195. Fax: 31 30 253 6723. E-mail: C.A.M.deHaan@uu.nl.

‡ M.H.V. and M.C.H. contributed equally to the article.

Present address: Pathology Division, Department of Pathobiology, Faculty of Veterinary Medicine, Utrecht University, Utrecht, The Netherlands.

† Supplemental material for this article may be found at <http://jvi.asm.org/>.

∇ Published ahead of print on 25 August 2010.

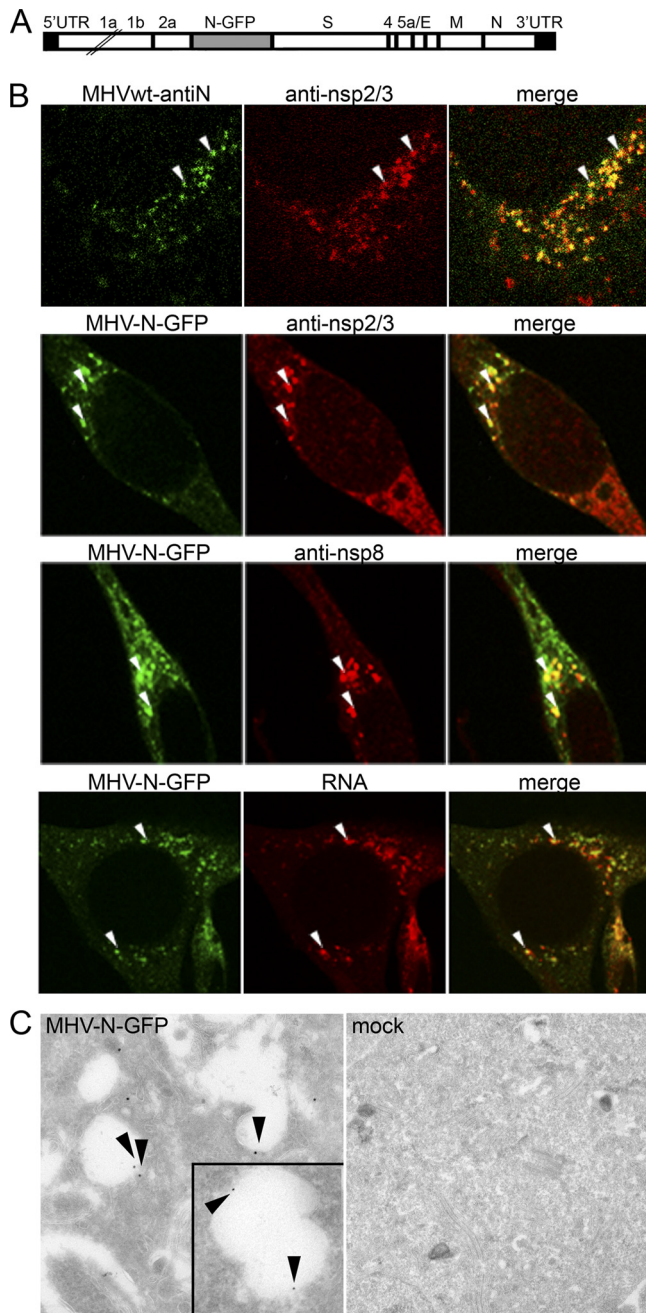


FIG. 1. Recruitment and localization of the N protein to the RTCs and DMVs. (A) Schematic outline of the MHV-N-GFP recombinant virus (not drawn to scale). UTR, untranslated region. (B) LR7 cells inoculated with MHV or MHV-N-GFP were fixed at 6 h p.i. and stained with antibodies directed against nsp2/3 (D4 [24]; kind gift of S. Baker) or nsp8 (anti-p22 antibody [15]; kind gift of M. Denison). Production of newly synthesized viral RNA was visualized by using Click-It detection of RNA. To this end, infected cells were fed with 5-ethynyl uridine from 5.5 to 6.5 h p.i., after which the cells were fixed. (C) HeLa-CEACAM1a cells infected with MHV-N-GFP and control cells (mock) were fixed at 6 h p.i. and processed for immunoelectron microscopy using antibodies against GFP. Arrowheads indicate colocalization sites between N-GFP and either RTC protein markers (B) or DMVs (C).

antibody). Similar colocalization of the N protein with nsp2/3 was observed in cells infected with wild-type MHV (Fig. 1B). To confirm the recruitment of N-GFP to the sites of viral RNA synthesis, we also studied the colocalization of N-GFP with newly synthesized viral RNA, using the Click-It RNA detection assay (Invitrogen). Essentially all N-GFP-positive foci were also positive for newly synthesized viral RNA. Subsequently, immunoelectron microscopy was performed on MHV-N-GFP-infected cells, with the GFP tag labeled as described before (10). Although only few gold particles per cell could be detected, the profiles clearly show that N-GFP localized to the DMVs (Fig. 1C), which appeared here as empty vesicles as observed before when using the same immunoelectron microscopy procedure (10, 28), as well as to the CMs (data not shown). All together, these results show that the N-GFP fusion proteins, when expressed from the viral genome, are recruited to the coronavirus replicative structures, which are corresponding with the active RTCs, similarly to the nontagged N protein (28).

To study the dynamics of the N protein association with the RTCs, we performed fluorescence recovery after photobleaching (FRAP) analysis of MHV-N-GFP-infected LR7 cells. At 6 h p.i., specific regions of interest (ROI) that contained one N-GFP-positive structure were irreversibly photobleached and recovery rates were determined as previously described (10). The photobleached N-GFP-positive structures had a reduction in signals to about 35% of that of the prebleached structures (Fig. 2A and D; see also Movie S1A in the supplemental material). Within 60 s, the signal at the ROI recovered to 60% of the original signal intensity, indicating an exchange of N-GFP with its surrounding environment. Recovery after photobleaching was also observed when N-GFP was expressed from a plasmid transfected into cells prior to infection with wild-type MHV (Fig. 2B and D; see also Movie S1B in the supplemental material). However, the mobility fraction (Mf) of N-GFP-positive foci in these cells was higher (Mf = 63%) than that of N-GFP in MHV-N-GFP-infected cells (Mf = 40%) (Fig. 2D). This might be attributed to the higher N-GFP expression levels in the transfected cells (compare Fig. 2A and B) (also data not shown). Although we previously did not observe any recovery of the nsp2-GFP signal in FRAP experiments (10) (Fig. 2D), we decided to simultaneously compare the recovery rates of N with those of nsp2 in the same cell. To this end, we cotransfected cells with plasmids expressing N-GFP and nsp2-mCherry (10) before infecting them with MHV. After subsequent infection with MHV, the N-GFP and nsp2-mCherry localized to partly overlapping cytoplasmic foci. Again, recovery of the N protein signal, but not that of nsp2, was detected after photobleaching (Fig. 2C; see also Movie S1C in the supplemental material), although the recovery of the N protein appeared to be less efficient than that in nsp2-mCherry-negative cells (Fig. 2B). This difference might be caused by differences in expression level. Alternatively, overexpression of nsp2 might affect the recovery of N-GFP, for instance, by yet-unrevealed protein-protein interactions. In conclusion, at 6 to 7 h p.i., the nsp2 and N protein present at the RTCs display different motilities, with the nsp2 being much less mobile in the cell than the N protein. It will be interesting to analyze the motility of the N protein at other time points of the infection cycle as well.

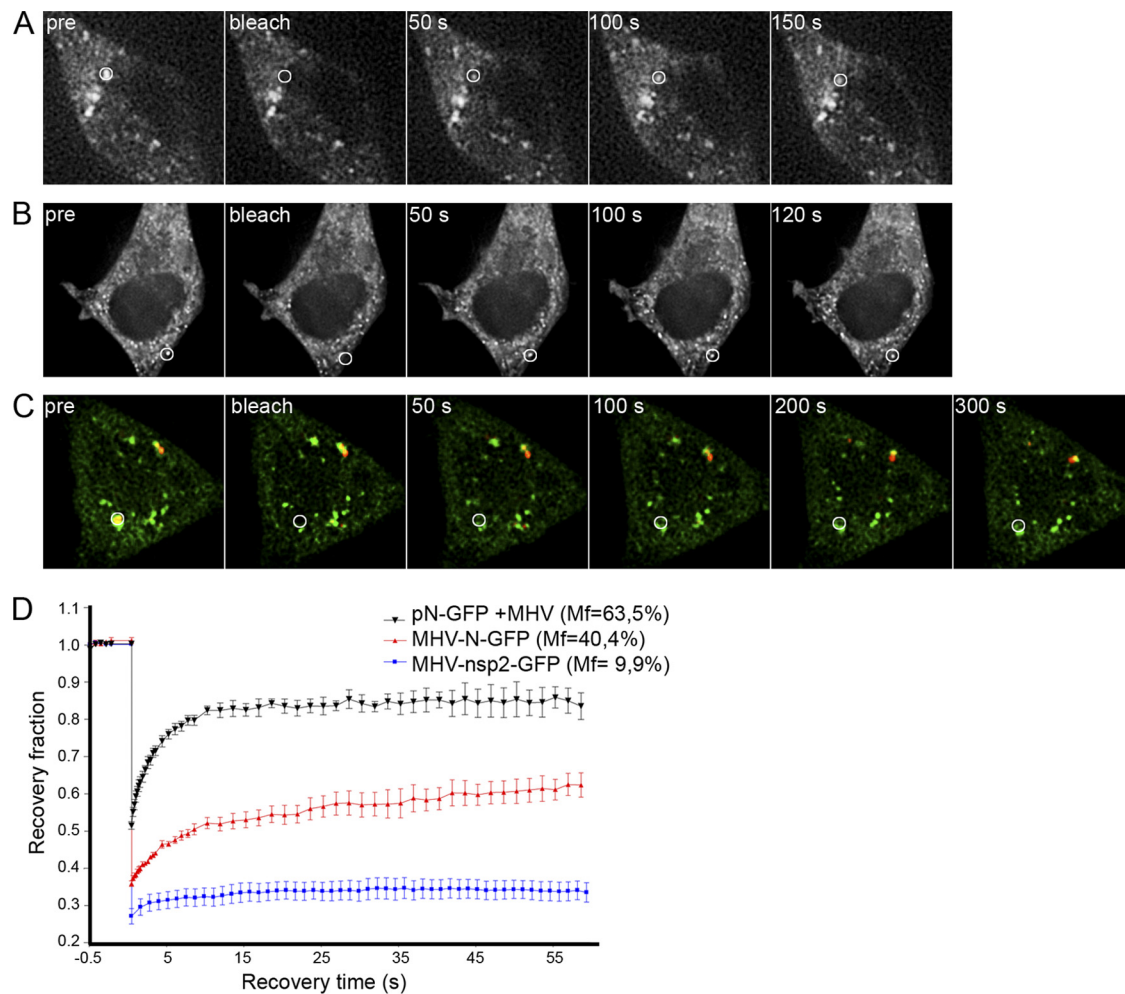


FIG. 2. Recovery of nucleocapsid protein N on DMVs after photobleaching. (A to C) FRAP was performed using the quantifiable laser module of the DeltaVision Core (API) at 6 h p.i. on LR7 cells infected with MHV-N-GFP (A), transfected with the N-GFP plasmid and subsequently infected with MHV-A59 (B), or cotransfected with pN-GFP (green) and pns2-mCherry (red) expression vectors and subsequently infected with MHV-A59 (C). Representative-experiment snapshots with the ROI indicated by white circles are depicted. (D) Fluorescence recovery graphs for photobleached ROIs from panels A ($n = 5$) and B ($n = 4$) are shown and compared with identically generated graphs for MHV-nsp2-GFP ($n = 10$) from a different study (10). Mf, mobile fraction, defined as the percentage of fluorescence recovery at the bleached site.

Next, we elucidated which part of the N protein is required for its dynamic recruitment to the RTCs. We made use of the recently described set of recombinant MHVs (12), each expressing, in addition to the full-length N protein, one of the following N-terminally GFP-tagged N segments: N1a (amino terminus), N1b (corresponding to the previously designated N-terminal domain [NTD]), N2a (region linking N1b and N2b), N2b (corresponding to the previously designated C-terminal domain [CTD]), and NBd3 (carboxyl terminus) (Fig. 3A) (see references in reference 12). We infected cells with these recombinant MHVs and analyzed at 6 h p.i. the recruitment of GFP-N domains to the RTCs after immunostaining them with antibodies directed against nsp8 (Fig. 3B). None of the N protein segments, with the exception of GFP-N2b (Fig. 3B), was efficiently recruited to the RTCs. As a result, the N2b domain probably contains the information required for recruitment of the N protein to the RTCs, at least in the presence of a full-length N protein. To a minor extent, some colocalization of GFP-N2a with nsp8 was also observed, which is in agree-

ment with this domain interacting with nsp3 (12a). Importantly, the FRAP experiments showed that the dynamic association/dissociation of GFP-N2b with the RTCs was similar to that of the full-length N-GFP (data not shown). Interestingly, all of the N protein segments except N2b also localized to the nucleus. Also, the full-length protein hardly localized to the nucleus (Fig. 1B). The biological significance of these observations is not clear at present.

The N2b segment has been demonstrated to be involved in both N protein self-interaction and binding to the RNA (see references in reference 12). To determine which of these two interactions is essential for the recruitment of the N2b fragment to the RTCs, we performed coimmunoprecipitation experiments. To this end, cells infected with the different recombinant MHVs were metabolically labeled as previously described (10) from 5 h to 7 h p.i. Subsequently, cell lysates were prepared and immunoprecipitations were performed essentially as described previously (31) either in the presence or absence of the anti-GFP antibody (Fig. 4A). When immuno-

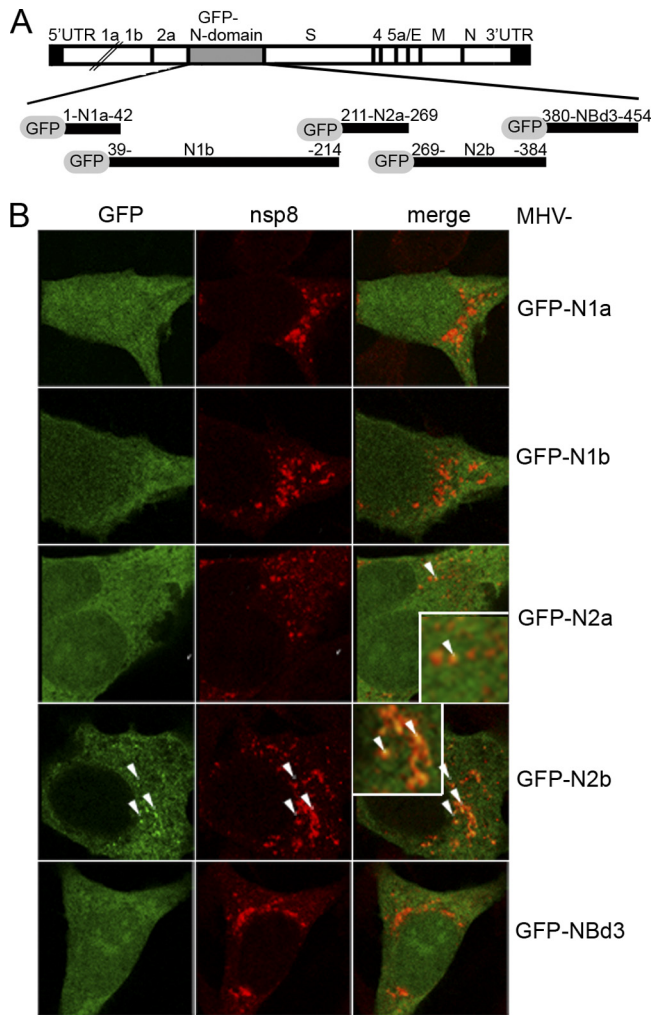


FIG. 3. Role of N domains in RTC recruitment. (A) Schematic outline of the MHV-GFP-N domain recombinant viruses (not drawn to scale). (B) LR7 cells infected with MHV-GFP-N domain viruses were fixed and processed for immunofluorescence at 6 h p.i. using the RTC protein marker nsp8. Examples of GFP-N2a and -N2b-positive foci colocalizing with nsp8 are indicated by arrowheads.

precipitations were performed in the absence of the anti-GFP antibody, very low levels of full-length N protein were detected, likely due to the nonspecific binding to protein A Sepharose. In the presence of anti-GFP antibody, protein bands corresponding to the different fusion proteins were observed. Importantly, wild-type, nontagged N protein was efficiently coimmunoprecipitated in cells infected with viruses expressing N-GFP, GFP-N1b, or GFP-N2b (Fig. 4A). Since GFP-N2b, but not GFP-N1b, was recruited to the RTCs (Fig. 3B), we subsequently investigated whether these interactions were dependent on the presence of viral RNA. To this end, the immunoprecipitates were treated with RNase A (17). As expected, the interaction between wild-type N protein and full-length N-GFP protein was lost after RNase A treatment (Fig. 4B) (17). The same result was obtained for the GFP-N1b protein, whereas for the GFP-N2b protein, the interaction with N was maintained after RNase A incubation (Fig. 4B).

In this study, we show that the N protein, in contrast to nsp2

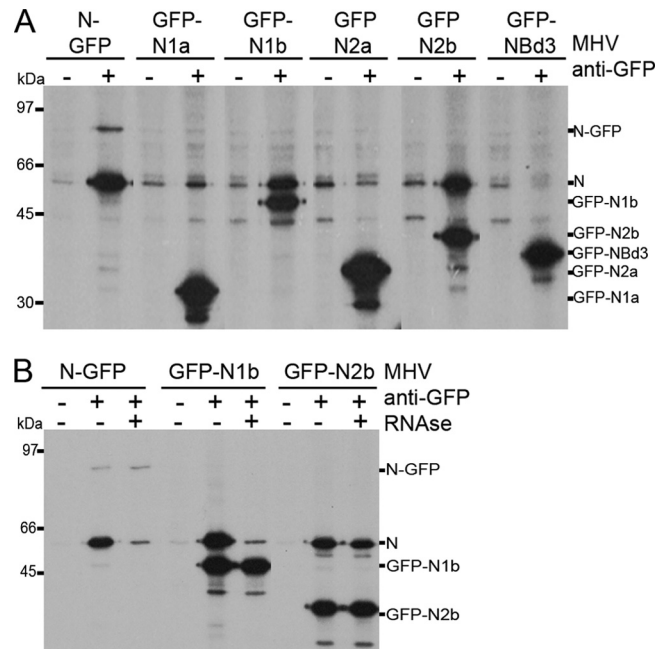


FIG. 4. Intracellular N-N interactions and their RNA dependency. LR7 cells were infected with MHV-GFP-N domain viruses and radioactively labeled from 5 h to 7 h p.i. before cell lysates were prepared. (A and B) Immunoprecipitations were performed in the absence (-) or presence (+) of GFP antibody (Immunology Consultants Laboratory, Inc.). Where indicated in panel B, the immunoprecipitates were treated with protease-free RNase A (Fermentas GmbH, St. Leon-Rot, Germany) and extensively washed prior to SDS-PAGE analysis. Of note, in the second lane in panels A and B, the small amount of coprecipitated N-GFP compared to that of nontagged N protein is likely due to only 10 to 20% of the MHV-N-GFP stock expressing N-GFP.

(10), is dynamically associated with the RTCs. The dynamics of other proteins present at the RTCs have not yet been evaluated. Whereas nsp2 may be immobilized within an elaborate network of protein-protein interactions (10, 19, 30), this is apparently not the case for the N protein. We hypothesize that the difference in mobility between nsp2 and N likely reflects their different functions in the viral life cycle. Although the function of nsp2 at the RTC is not known, the N protein is a multifunctional protein that facilitates RNA synthesis but also plays an essential role in virus assembly and is presumably involved in facilitating the transport of the viral genome from its location of synthesis to the virion assembly sites. The dynamic nature of the N protein at the RTCs may be a prerequisite for the N protein to exert and coordinate its diverse functions.

The N2b domain appeared to be required for N protein recruitment to the RTCs and was furthermore engaged in RNA-independent N-N interactions. The latter observation is consistent with previous studies that showed the importance of the CTD domain in N protein self-interactions (4, 8, 11, 13, 21, 32). Conceivably, GFP-N2b is recruited to the RTCs by binding a wild-type N protein molecule. We can, however, not rule out that its association with the DMVs is mediated by another RTC component. Strikingly, in contrast to N1b and NBd3, the N2b domain hardly appeared to be incorporated into progeny

virions (12). This was ascribed to its presumed inability to compete with full-length N monomers as the nucleocapsid condenses to be incorporated into the budding virion. Another explanation might be that RNA binding is an essential requirement for incorporation of N into virions, a feature the N2b did not seem to possess (12). Apparently, different N protein requirements exist with respect to its recruitment to the RTCs (this study) and its incorporation into virus particles (12). Differences in protein behavior are also observed between GFP-N2b and N-GFP. While the full-length N-GFP protein was efficiently recruited to the RTCs, more so than with GFP-N2b (compare Fig. 1B and 3B), its interaction with wild-type N protein was largely sensitive to RNase A treatment in the same manner as was GFP-N1b, which was not recruited to the RTCs. We speculate that while protein-protein interactions between N molecules are required for RTC recruitment, these interactions are somehow additionally influenced or converted by the presence of other N protein domains, for example, via N-RNA interactions.

We thank Corlinda ten Brink (Department of Cell Biology and the Cell Microscopy Center, University Medical Centre Utrecht) and Colleen O'Hare (Applied Precision, Inc.) for technical support. We thank Susan Baker and Mark Denison for providing antibodies.

This work was supported by grants from the Netherlands Organization for Scientific Research (NWO-VIDI) and the Utrecht University (High Potential) to C. A. M. de Haan and F. Reggiori.

REFERENCES

- Ahluquist, P., A. O. Noueiry, W. M. Lee, D. B. Kushner, and B. T. Dye. 2003. Host factors in positive-strand RNA virus genome replication. *J. Virol.* **77**:8181–8186.
- Baric, R. S., G. W. Nelson, J. O. Fleming, R. J. Deans, J. G. Keck, N. Casteel, and S. A. Stohlman. 1988. Interactions between coronavirus nucleocapsid protein and viral RNAs: implications for viral transcription. *J. Virol.* **62**:4280–4287.
- Bost, A. G., R. H. Carnahan, X. T. Lu, and M. R. Denison. 2000. Four proteins processed from the replicase gene polyprotein of mouse hepatitis virus colocalize in the cell periphery and adjacent to sites of virion assembly. *J. Virol.* **74**:3379–3387.
- Chang, C. K., S. C. Sue, T. H. Yu, C. M. Hsieh, C. K. Tsai, Y. C. Chiang, S. J. Lee, H. H. Hsiao, W. J. Wu, W. L. Chang, C. H. Lin, and T. H. Huang. 2006. Modular organization of SARS coronavirus nucleocapsid protein. *J. Biomed. Sci.* **13**:59–72.
- Compton, S. R., D. B. Rogers, K. V. Holmes, D. Fertsch, J. Remenick, and J. J. McGowan. 1987. In vitro replication of mouse hepatitis virus strain A59. *J. Virol.* **61**:1814–1820.
- de Haan, C. A., and P. J. Rottier. 2005. Molecular interactions in the assembly of coronaviruses. *Adv. Virus Res.* **64**:165–230.
- Denison, M. R., W. J. Spaan, Y. van der Meer, C. A. Gibson, A. C. Sims, E. Prentice, and X. T. Lu. 1999. The putative helicase of the coronavirus mouse hepatitis virus is processed from the replicase gene polyprotein and localizes in complexes that are active in viral RNA synthesis. *J. Virol.* **73**:6862–6871.
- Fan, H., A. Ooi, Y. W. Tan, S. Wang, S. Fang, D. X. Liu, and J. Lescar. 2005. The nucleocapsid protein of coronavirus infectious bronchitis virus: crystal structure of its N-terminal domain and multimerization properties. *Structure* **13**:1859–1868.
- Gosert, R., A. Kanjanahaluthai, D. Egger, K. Bienz, and S. C. Baker. 2002. RNA replication of mouse hepatitis virus takes place at double-membrane vesicles. *J. Virol.* **76**:3697–3708.
- Hagemeyer, M. C., M. H. Verheije, M. Ulasli, I. A. Shaltiel, L. A. de Vries, F. Reggiori, P. J. Rottier, and C. A. M. de Haan. 2010. Dynamics of coronavirus replication-transcription complexes. *J. Virol.* **84**:2134–2149.
- Huang, C. Y., Y. L. Hsu, W. L. Chiang, and M. H. Hou. 2009. Elucidation of the stability and functional regions of the human coronavirus OC43 nucleocapsid protein. *Protein Sci.* **18**:2209–2218.
- Hurst, K. R., C. A. Koetznner, and P. S. Masters. 2009. Identification of in vivo-interacting domains of the murine coronavirus nucleocapsid protein. *J. Virol.* **83**:7221–7234.
- Hurst, K. R., R. Ye, S. F. Goebel, P. Jayaraman, and P. S. Masters. 2010. An interaction between the nucleocapsid protein and a component of the replicase-transcriptase complex is crucial for the infectivity of coronavirus genomic RNA. *J. Virol.* **84**:10276–10288.
- Jayaram, H., H. Fan, B. R. Bowman, A. Ooi, J. Jayaram, E. W. Collisson, J. Lescar, and B. V. Prasad. 2006. X-ray structures of the N- and C-terminal domains of a coronavirus nucleocapsid protein: implications for nucleocapsid formation. *J. Virol.* **80**:6612–6620.
- Knoops, K., M. Kikkert, S. H. Worm, J. C. Zevenhoven-Dobbe, Y. van der Meer, A. J. Koster, A. M. Mommaas, and E. J. Snijder. 2008. SARS-coronavirus replication is supported by a reticulovesicular network of modified endoplasmic reticulum. *PLoS Biol.* **6**:e226.
- Lu, X. T., A. C. Sims, and M. R. Denison. 1998. Mouse hepatitis virus 3C-like protease cleaves a 22-kilodalton protein from the open reading frame 1a polyprotein in virus-infected cells and in vitro. *J. Virol.* **72**:2265–2271.
- Mizutani, T., A. Maeda, M. Hayashi, H. Isogai, and S. Namioka. 1994. Both antisense and sense RNAs against the nucleocapsid protein gene inhibit the multiplication of mouse hepatitis virus. *J. Vet. Med. Sci.* **56**:211–215.
- Narayanan, K., K. H. Kim, and S. Makino. 2003. Characterization of N protein self-association in coronavirus ribonucleoprotein complexes. *Virus Res.* **98**:131–140.
- Oostra, M., E. G. te Lintelo, M. Deijis, M. H. Verheije, P. J. M. Rottier, and C. A. M. de Haan. 2007. Localization and membrane topology of the coronavirus nonstructural protein 4: involvement of the early secretory pathway in replication. *J. Virol.* **81**:12323–12336.
- Pan, J., X. Peng, Y. Gao, Z. Li, X. Lu, Y. Chen, M. Ishaq, D. Liu, M. L. Dediego, L. Enjuanes, and D. Guo. 2008. Genome-wide analysis of protein-protein interactions and involvement of viral proteins in SARS-CoV replication. *PLoS One* **3**:e3299.
- Prentice, E., W. G. Jerome, T. Yoshimori, N. Mizushima, and M. R. Denison. 2004. Coronavirus replication complex formation utilizes components of cellular autophagy. *J. Biol. Chem.* **279**:10136–10141.
- Saikatendu, K. S., J. S. Joseph, V. Subramanian, B. W. Neuman, M. J. Buchmeier, R. C. Stevens, and P. Kuhn. 2007. Ribonucleocapsid formation of severe acute respiratory syndrome coronavirus through molecular action of the N-terminal domain of N protein. *J. Virol.* **81**:3913–3921.
- Sawicki, S. G., D. L. Sawicki, and S. G. Siddell. 2007. A contemporary view of coronavirus transcription. *J. Virol.* **81**:20–29.
- Shi, S. T., and M. M. Lai. 2005. Viral and cellular proteins involved in coronavirus replication. *Curr. Top. Microbiol. Immunol.* **287**:95–131.
- Shi, S. T., J. J. Schiller, A. Kanjanahaluthai, S. C. Baker, J. W. Oh, and M. M. Lai. 1999. Colocalization and membrane association of murine hepatitis virus gene 1 products and de novo-synthesized viral RNA in infected cells. *J. Virol.* **73**:5957–5969.
- Snijder, E. J., Y. van der Meer, J. Zevenhoven-Dobbe, J. J. Onderwater, J. van der Meulen, H. K. Koerten, and A. M. Mommaas. 2006. Ultrastructure and origin of membrane vesicles associated with the severe acute respiratory syndrome coronavirus replication complex. *J. Virol.* **80**:5927–5940.
- Stertz, S., M. Reichelt, M. Spiegel, T. Kuri, L. Martinez-Sobrido, A. Garcia-Sastre, F. Weber, and G. Kochs. 2007. The intracellular sites of early replication and budding of SARS-coronavirus. *Virology* **361**:304–315.
- Surjit, M., and S. K. Lal. 2008. The SARS-CoV nucleocapsid protein: a protein with multifarious activities. *Infect. Genet. Evol.* **8**:397–405.
- Ulasli, M., M. H. Verheije, C. A. de Haan, and F. Reggiori. 2010. Qualitative and quantitative ultrastructural analysis of the membrane rearrangements induced by coronavirus. *Cell Microbiol.* **12**:844–861.
- Verheije, M. H., M. Raaben, M. Mari, E. G. Te Lintelo, F. Reggiori, F. J. van Kuppeveld, P. J. Rottier, and C. A. de Haan. 2008. Mouse hepatitis coronavirus RNA replication depends on GBF1-mediated ARF1 activation. *PLoS Pathog.* **4**:e1000088.
- von Brunn, A., C. Teepe, J. C. Simpson, R. Pepperkok, C. C. Friedel, R. Zimmer, R. Roberts, R. Baric, and J. Haas. 2007. Analysis of intraviral protein-protein interactions of the SARS coronavirus ORF3e. *PLoS One* **2**:e459.
- Wessels, E., D. Duijsings, R. A. Notebaart, W. J. Melchers, and F. J. van Kuppeveld. 2005. A proline-rich region in the coxsackievirus 3A protein is required for the protein to inhibit endoplasmic reticulum-to-Golgi transport. *J. Virol.* **79**:5163–5173.
- Yu, I. M., M. L. Oldham, J. Zhang, and J. Chen. 2006. Crystal structure of the severe acute respiratory syndrome (SARS) coronavirus nucleocapsid protein dimerization domain reveals evolutionary linkage between *Coronae* and *Arteriviridae*. *J. Biol. Chem.* **281**:17134–17139.
- Zuniga, S., I. Sola, J. L. Moreno, P. Sabella, J. Plana-Duran, and L. Enjuanes. 2007. Coronavirus nucleocapsid protein is an RNA chaperone. *Virology* **357**:215–227.